ROTATING-BENDING FATIGUE OF A TiNi SHAPE-MEMORY ALLOY WIRE

H. Tobushi and T. Hachisuka
Department of Mechanical Engineering, Aichi Institute of Technology, Toyota, 470-03, Japan

S. Yamada
Sato Kogyo, Ltd., Tokyo, 103, Japan

P. H. Lin
Department of Mechanical Engineering, Southeast University, Nanjing, 210096, China

ABSTRACT

The rotating-bending fatigue of a TiNi shape-memory alloy wire was investigated. Influence of air and water atmospheres, temperature, strain amplitude and rotational speed on fatigue life was discussed. In the case of the strain amplitude due to the rhombohedral-phase transformation, the fatigue life lengthened above 10^7 cycles. In the case of the strain amplitude due to the martensitic transformation, the fatigue life in air shortened under that in water.

KEYWORDS

Shape memory alloy, Titanium-Nickel alloy, fatigue, rotating-bending, wire, rotational speed, atmosphere

INTRODUCTION

The shape memory effect (SME) and the superelasticity (SE) appear in shape memory alloy (SMA). In TiNi SMA, these properties occur due to the martensitic transformation (MT) and the rhombohedral-phase transformation (RPT). If SMAs are applied to the working elements of an actuator, a robot and a solid-state heat engine, SMAs perform cyclic motions. In order to evaluate the reliability of memory elements, cyclic deformation properties of SMAs are important (Tobushi et al., 1991; Tobushi et al., 1995). If we use SMAs under high cycles in actuators, robots and solid-state heat engines, fatigue of SMAs is an important problem in order to develop these devices (McNichols et al., 1981; Melton and Mercier, 1979; Miyazaki, 1990).

In SMAs, fatigue limit of TiNi SMA is high because the grain size is small. Because the response property of SMA elements is determined based on the property of heat transfer, a thin wire is most widely used in applications. In a simple-pulley heat engine (Tobushi et al., 1990), a SMA element performs cyclic bending. In order to evaluate the fatigue property in these cases, it is necessary to carry out the rotating-bending test on the wire.

In the present study, a rotating-bending fatigue test machine for the SMA wire was developed. Influence of air and water atmospheres, strain amplitude, temperature and rotational speed on fatigue of the TiNi SMA wire was investigated.

EXPERIMENTAL METHOD

Material and Specimen

Material was a Ti-55.3wt%Ni SMA wire, 0.75mm in diameter. A straight line was shape-memorized through shape memory processing by keeping at 673K for one hour followed by cooling in a furnace. The grain size was from submicron to several microns. The A_f point of a specimen determined by tensile test was about 323K. The length of the specimen was 155-255mm. The distance between supports was 65-165mm. The larger the curvature of bending of the specimen, the shorter the distance between supports and the length of the specimen.

Experimental Apparatus

The experimental apparatus for the rotating-bending test of the wire is shown in Fig.1. The apparatus was composed of a working part to perform rotating-bending and a chamber or a water bath to keep temperature constant. One end of the specimen was mounted to a motor and the other end rotated freely at which the number of cycles to failure was measured. In order to avoid torsional moment, ball bearings were used at the supports of both ends. The specimen was in air or in water.

The curvature of the specimen was determined as follows. Before the test, the bent form of the specimen was traced on a section paper. After the test, the radius of curvature of a ruptured part was measured. Using the radius of curvature, maximum strain on the surface of the specimen was obtained.

Experimental Procedure

The rotating-bending test was performed in air and in water. In the experiment, the influence of air and water atmospheres, the maximum strain on the surface of the specimen (strain amplitude) ε_a, temperature T and rotational speed n on fatigue was investigated. The strain amplitude was 0.5-2.5%. Temperature was room temperature (RT) in air, 303K,333K and 353K. Rotational speed was 100-1000rpm. In the case of RT in air, temperature was not controlled.

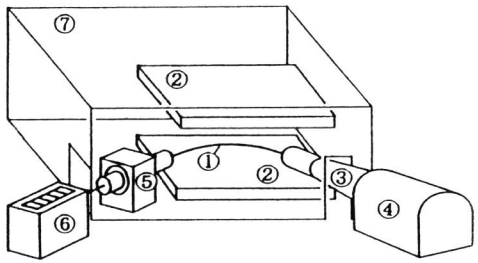

(a) Setup for the fatigue test in air

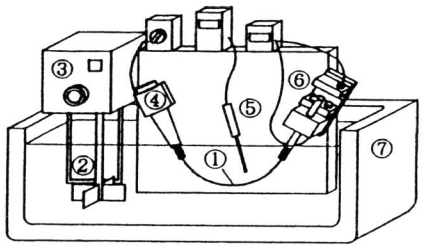

(b) Setup for the fatigue test in water

Fig.1 Experimental apparatus

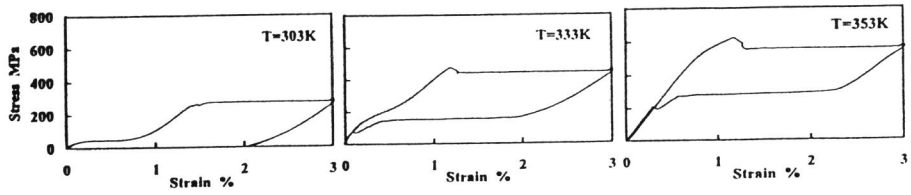

Fig.2 Stress-strain curves

In order to obtain the stress-strain relationship due to MT and RPT, the tensile test at various temperatures was carried out.

EXPERIMENTAL RESULTS AND DISCUSSION

Deformation Properties

The stress-strain curves obtained by the tensile test at various temperatures T are shown in Fig.2. As seen Fig.2, in the case of T=303K below A_f, yielding due to RPT occurs under stress of 50MPa. The yielding due to RPT starts at strain of 0.2% and completes at 0.8%. After RPT, yielding due to MT occurs at strain of 1.4% under stress of 250MPa. In this case, residual strain appears after unloading. The residual strain disappears by heating above A_f under no stress. This phenomenon is SME. In the case of T=333K and 353K above A_f, yield stress due to both transformations increases in proportion to temperature. The reverse transformation occurs and strain is recovered during the unloading process. This phenomenon is SE. In the case of T=353K, RPT does not appear and only MT appears.

Stress Distribution Under Bending

The stress distribution in a cross section and the transformed region in a longitudinal section of a wire which is subjected to bending are schematically shown in Fig.3. The stress distribution and the transformed region are determined based on the deformation properties of the material shown in Fig.2. As seen in Fig.3, central part is elastic region and the transformed region expands from surface area to the central part as the bending strain increases. In the surface area, RPT occurs at first and thereafter MT occurs as the

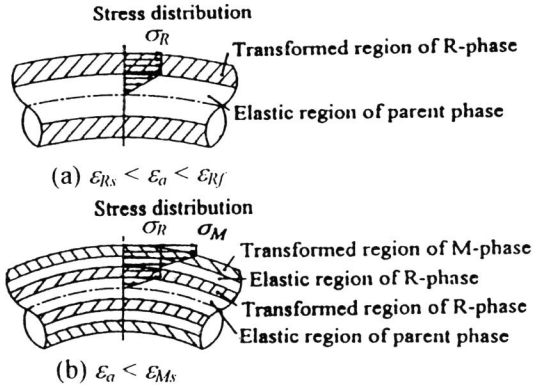

Fig.3 Stress distribution and transformed region in the wire under bending

curvature of bending increases. If the wire makes one revolution by keeping the bent form, the element in the surface area is subjected to tension and compression. Therefore, in the fatigue test, the element in the surface area is subjected to cyclic transformation due to tension and compression.

Temperature Rise in Air

The relationship between temperature rise ΔT and time t obtained by the fatigue test at room temperature with various strain amplitudes ε_a under a constant rotational speed n=300rpm in air is shown in Fig.4. As seen in Fig.4, ΔT increases rapidly in the early cycles but takes almost a constant value after 150 seconds. ΔT increases in proportion to ε_a. The relationship between the maximum saturated value ΔT_m and n is shown in Fig.5. As seen in Fig.5, the larger the n, the larger the ΔT_m. The dependence of ΔT_m on ε_a and n is explained as follows. As seen in Fig.2, the stress-strain curve draws a hysteresis loop. The area surrounded by the hysteresis loop denotes dissipated strain energy per unit volume E_d. Based on E_d which appears in each cycle, temperature rises. Because E_d is determined by the product of stress and strain, E_d increases in proportion to ε_a. If E_d is balanced with heat conduction and radiant heat, ΔT is saturated to ΔT_m. If strain rate is larger than 10%/min, yield stress due to MT increases in proportion to strain rate (Lin et al., 1996). Therefore, if n is large, E_d is large. Because ΔT increases as E_d increases, ΔT_m is large in proportion to n.

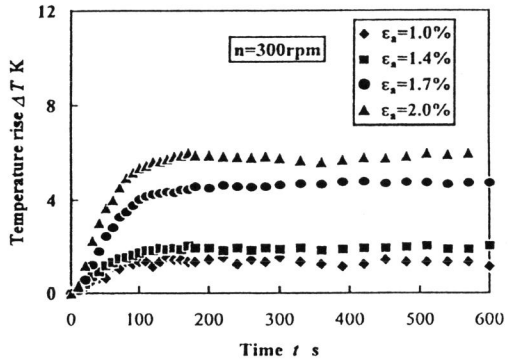

Fig.4 Relationship between temperature rise ΔT and time t in air

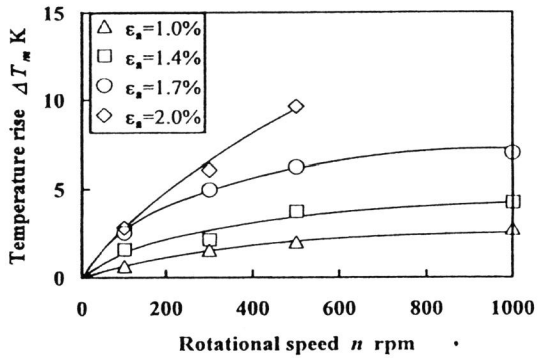

Fig.5 Relationship between maximum temperature rise ΔT_m and rotational speed n

Fatigue Properties

(1) Fatigue in air

The relationship between the strain amplitude ε_a and the number of cycles to failure N_f obtained by fatigue test at various temperatures T under a constant rotational speed n=500rpm in air is shown in Fig.6. In the case of N_f=10^6 plotted with an arrow, the specimen was not ruptured. As seen in Fig.6, in the case that ε_a is larger than 0.8%, N_f is small in proportion to ε_a. The relationship between ε_a and

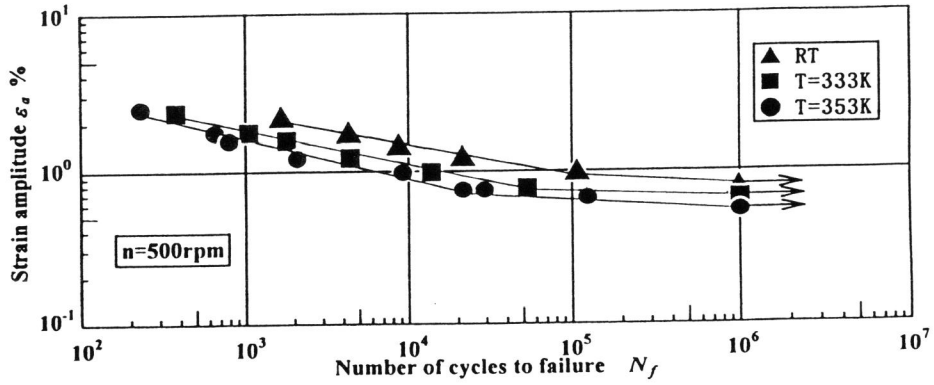

Fig.6 Relationship between strain amplitude and the number of cycles to failure at various temperatures in air

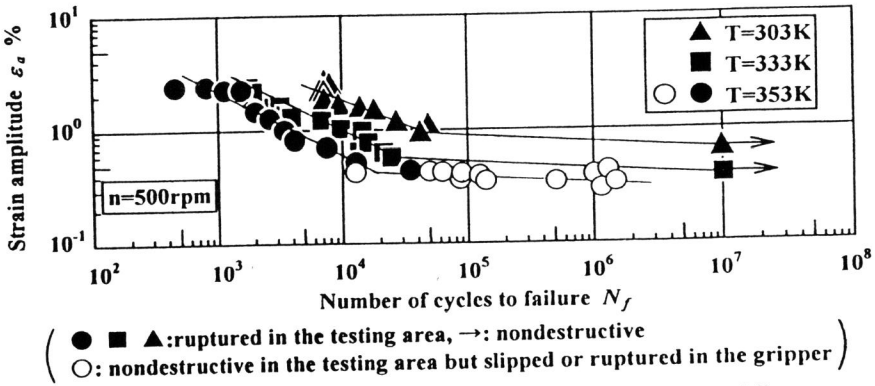

Fig.7 Relationship between strain amplitude and the number of cycles to failure at various temperatures in water

N_f in this region is expressed by a linear line. The slope of the straight line coincides at each temperature. If the straight line is expressed by the equation

$$\varepsilon_a = \alpha \cdot N_f^{-\beta}, \quad \cdots\cdots(1)$$

a value of β is 0.235. This value is smaller than β=0.5 which is valid for normal metals. Equation (1) corresponds to the Manson-Coffin relationship between fatigue life and total strain in low cycle fatigue. The reason why β is small is explained as follows. As seen in Fig.4, ΔT is large in proportion to ε_a. Yield stresses due to MT and RPT increase in proportion to temperature. Therefore, in the case of large ε_a, stress is high, resulting in small N_f. As the result of small N_f for large ε_a, β is small.

In the region of ε_a=0.8-1% or N_f=10^4-10^5, the ε_a-N_f curve has a knee. In the case that ε_a is smaller

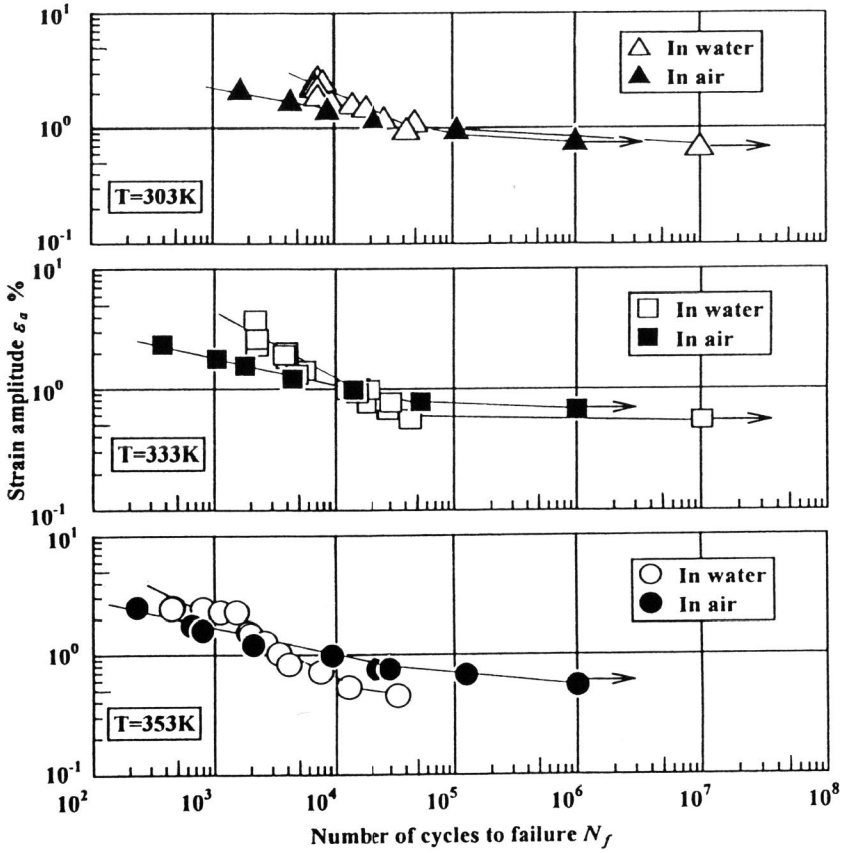

Fig.8 Relationship between strain amplitude and the number of cycles to failure at various temperatures in air and in water

than 0.8%, N_f increases significantly and the curve approaches a horizontal line. The region of ε_a below 0.8% corresponds to RPT. Therefore, in applications of SMAs, fatigue life is quite long if TiNi SMA is used in the region of RPT.

If temperature T is high, the curve moves to the left and downward. That is, the higher the T, the smaller the N_f for the same ε_a. This is due to the fact that yield stresses due to MT and RPT are high in proportion to T, resulting in small N_f.

(2) Fatigue in water

The relationship between ε_a and N_f obtained by fatigue test at various temperatures T under constant n=500rpm in water is shown in Fig.7. As seen in Fig.7, the overall inclination of the relationship is the same as that in air shown in Fig.6. The slope of the curve represented by β in Eq.(1) in the region of large ε_a is 0.47. The value of β=0.47 is larger than that in air, but is close to 0.5 which is valid for normal metals. In the case of fatigue test in water, temperature of the wire does not increase but is kept constant. Therefore yield stress is constant during the fatigue test. In the case of normal metals in air, yield stress and plastic deformation properties do not change even if temperature increases by 10K. Therefore the value of β is about 0.5 in the case of normal metals and TiNi SMA in water. As seen in Fig.7, in the region of small ε_a where RPT occurs, fatigue life lengthens above 10^7 cycles.

(3) Influence of air and water atmospheres

The relationship between ε_a and N_f obtained by fatigue test at the same temperatures T in air and in water is shown in Fig.8. As seen in Fig.8, in the region of low cycle fatigue under 10^4 cycles, N_f in air is small and the slope of the straight line β is small. As mentioned above, the transformation start line for MT is expressed by (Tanaka et al., 1986)

$$\sigma = C_M(T - M_s) \quad \cdots\cdot(2)$$

and that for RPT by (Tobushi et al., 1992)

$$\sigma = C_R(T - M_R) \quad \cdots\cdot(3)$$

where σ represents stress. M_s and M_R represent the transformation start temperatures of MT and RPT under no stress, respectively. C_M and C_R denote the slopes of the transformation start lines. For TiNi SMA, C_M=6MPa/K and C_R=15MPa/K. Therefore, if ΔT=10K, the increase in MT stress is 60MPa and that in RPT 150MPa. If stress in the surface of a wire is high, initiation of fatigue crack is early, resulting in small N_f and small β in air. On the contrary, temperature does not change in water. In the

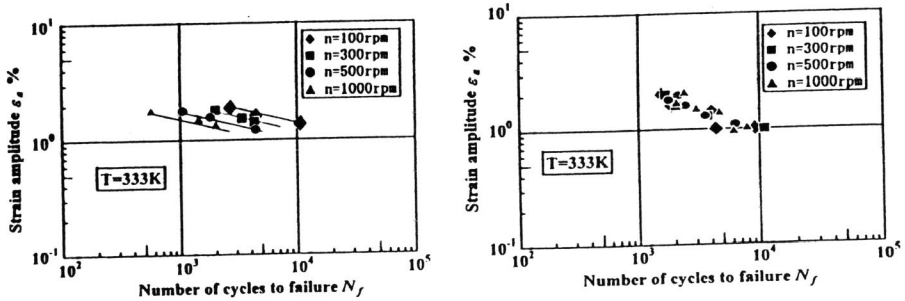

(a) In air (b) In water

Fig.9 Relationship between strain amplitude and the number of cycles to failure at various rotational speeds

case of normal metals, even if temperature rises by 10K around room temperature, yield stress and plastic deformation property do not change so sensitively as SMAs. Therefore the value of β is about 0.5 for SMA in water and normal metals.

As seen in Fig.8, the ε_a-N_f curves in air and in water intersect around the point of ε_a=1%. In the region of high cycle fatigue above 10^5 cycles, the ε_a-N_f curves in air and in water approach horizontal lines. In the region of high cycle fatigue, N_f in water shortens than that in air. This may occur due to corrosion fatigue of the wire in water.

(4) Influence of rotational speed

The relationship between ε_a and N_f obtained by fatigue test at various rotational speeds n in air and in water is shown in Fig.9. As seen in Fig.9, in water, the data at various n lie on almost the same line. In air, the larger the n, the smaller the N_f. As observed in Fig.5, if n is large, ΔT_m is large. Therefore, if n is large, the transformation stress is high, resulting in small N_f. In the case in water, temperature does not change even if n is different, resulting in the same N_f.

CONCLUSIONS

The rotating-bending fatigue test machine for the SMA wire was developed and the fatigue properties of the TiNi SMA wire were investigated. The results are summarized as follows.

(1) During the rotating-bending process in air, temperature rises. The temperature rise is proportional to the strain amplitude and the rotational speed. The fatigue life shortens due to the temperature rise.

(2) If the strain amplitude is in the region of MT, the fatigue life in air shortens than that in water.

(3) If the strain amplitude is in the region of RPT, the fatigue life lengthens above 10^7 cycles.

(4) The higher the temperature, the shorter the fatigue life.

REFERENCES

Lin, P. H., H. Tobushi, K. Tanaka, T. Hattori and A. Ikai (1996), JSME Inter. J., Ser. A, **39**-1, 117-123.

McNichols, Jr. J. L., P. C. Brookes and J. S. Cory (1981), J. Appl. Phys., **52**-12, 7442-7444.

Melton, K. N. and O. Mercier (1979), Acta Met., **27**, 137-144.

Miyazaki, S. (1990), Engineering Aspects of Shape Memory Alloys (T. W. Duerig, K. N. Melton, D. Stockel and C. M. Wayman ed.), 394-413, Butterworth-Heinemann.

Tanaka, K., S. Kobayashi and Y. Sato (1986), Inter. J. Plasticity, **2**, 59-72.

Tobushi, H., P. H. Lin, T. Hattori and M. Makita (1995), JSME Inter. J., Ser. A, **35**-1, 59-67.

Tobushi, H., K. Kimura, H. Iwanaga and J. R. Cahoon (1990), JSME Inter. J., Ser. I, **33**-2, 263-268.

Tobushi, H., H. Iwanaga, K. Tanaka, T. Hori and T. Sawada (1991), Continuum Mech. Thermodyn., **3**, 79-93.

Tobushi, H., K. Tanaka, K. Kimura, T. Hori and T. Sawada (1992), JSME Inter. J., Ser. I, **35**-3, 278-284.